Alkaline basic dykes in the central part of Sanandaj-Sirjan zone (Iran)

Mortaza Sharifi[1], Mohammad Sayari[1]*

1- Department of Geology, Faculty of Science, University of Isfahan, Isfahan, Iran.

* Corresponding Author: m.sayari@gmail.com

Received: 5 May 2013 / Accepted: 1 June 2013 / Published online: 3 June 2013

Abstract

There are three different basic dykes in the northeast of Golpayegan area, central part of Sanandaj-Sirjan Zone (SSZ) including: mylonitic gabbros (group 1), alkali dioritic-basanitic dykes (group 2) and alkali monzogabbroic to monzodioritic dykes (group 3). Group 2 and 3 cut post-collisional rocks and are related to after subduction processes of Neo-Tethys. Geochemistry characteristic of studied rocks indicate that group 2 is alkali basalt and two other groups are subalkali basalt-basaltic andesi. Group 2 and 3 are derived from an enriched mantle source. Group 2 is more enriched in HFSE, LILE and REE rather than other groups indicating that its source should be more enriched than group 1 and 3's. It can be inferred that magma forming rocks of group 2 was derived from an asthenospheric mantle, while magma forming two other groups was resulted from a lithospheric mantle. Magmas forming dykes were generated by intermediate degrees of partial melting (about 7-20% and 12-20% for group 2 and 3 respectively). Source of magma was maybe a peridotite which was previously metasomatised. It is probable that the cause of metasomatism in the source was the subducted slab related to subduction of Neo-Tethys beneath the studied area.

Keywords: Basic dykes; Subduction; Trace elements; Golpayegan; Sanandaj-Sirjan Zone; Tectonic setting.

1- Introduction

Historical events of geological evolution may be inferred from characteristics of magmatic rocks intruded or extruded in a region. Basic magmas are primitive or slightly changed primitive magmas which formed by partial melting of a peridotitic source under mantle conditions. Alkaline basic rocks present very useful data about the mineralogical and geochemical characteristics of mantle. They are supposed to be derived from partial melting of asthenospheric and/or lithospheric mantle (Pilet *et al*., 2005; Tang *et al*., 2006; Yan and Zhao, 2008). Alkali basalts occur in a great variety of oceanic and continental tectonic settings. These rocks are typically observed on updomed and rifted continental crust, and on oceanic islands (Turner and Hawkesworth, 1995). Alkali basalts contain compositional and thermal characteristics of their mantle sources and are indicators of tectonic regimes. They are commonly ascribed to convective mantle plumes or isentropic decompression induced by lithosphere stretching (Coban, 2007).

In Golpayegan area (western part of Isfahan province, Iran) located in Sanandaj-Sirjan Zone (Fig. 1), three groups of basic dykes intruded through the older lithology are exposed. These dykes form small masses which are observed within mylonitic-granitoids, mylonitic syenitic- dioritic rocks and Barrovian type metamorphic complex (Sharifi, 2008).

Group 1 from the basic dykes cropped out in north of the Varzaneh, groups 2 and 3 are exposed in the Sfajerd and Saeid-Abad in the northeast of the Golpayegan (Fig. 2). Applying $^{40}Ar/^{39}Ar$ dating, Moritz *et al*. (2006) estimated the age of biotite and amphibole in syentic-dioritic rocks at 54.85 ± 1.00 and 54.64 ± 1.66 Ma, respectively. Sharifi (2008) showed these rocks are post-collisional. Cutting syentic-dioritic rocks, group 2 and 3 are younger than age of 55 Ma and related to after subduction.

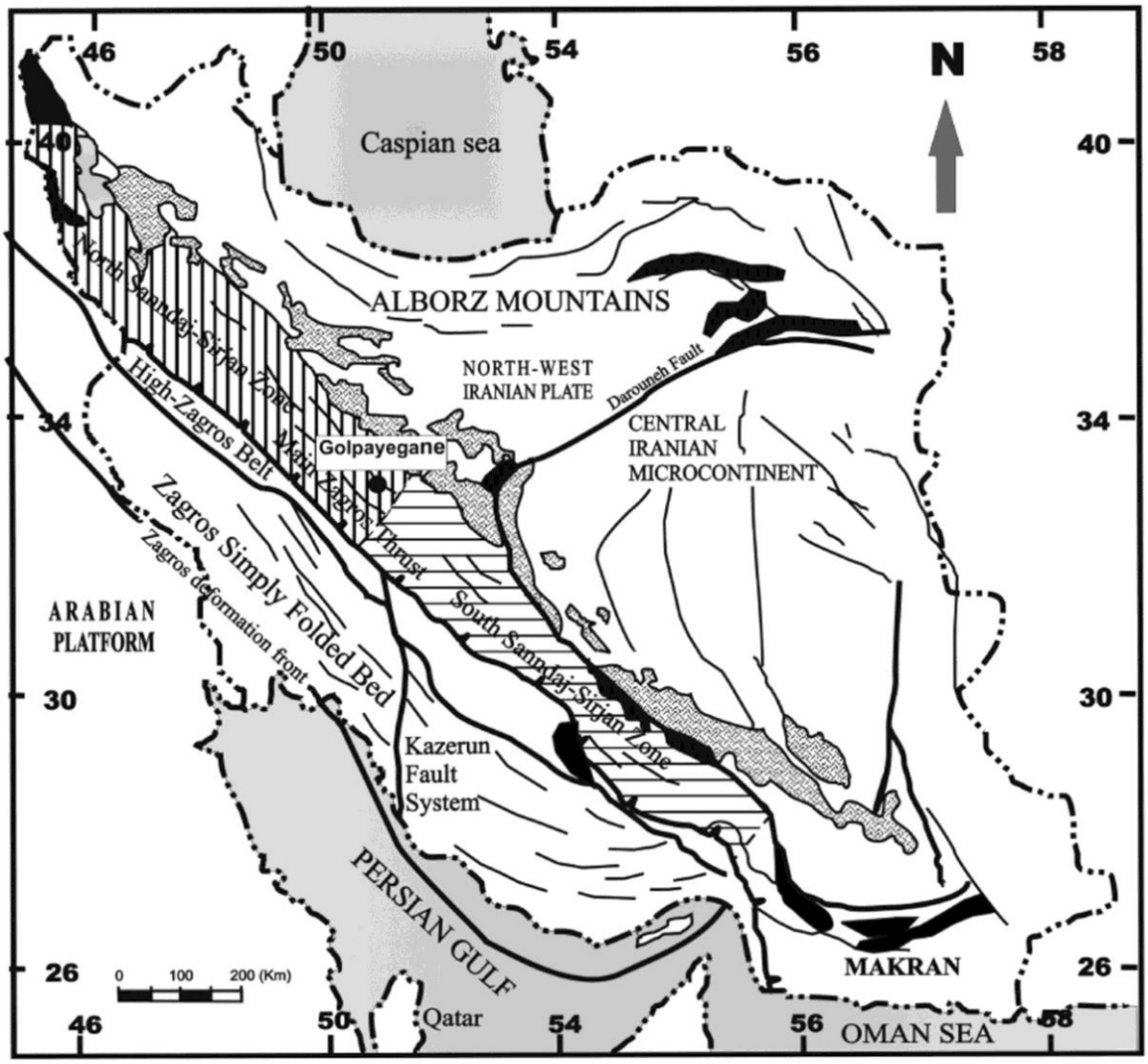

Figure 1) Main tectonic units of Iran and location of the study area in the Sanandaj-Sirjan Zone.

Golpayegan area is structurally located in Sanandaj-Sirjan Zone (SSZ) situated in central part of Iran (Fig. 1). SSZ has undergone complex geological and tectonical scenario that is a matter of controversy. It is approximately unanimously accepted that SSZ has experienced subduction of Neo-Tethys

Ocean even though the chronological events of tectonic setting and the kind of subduction has been a matter of controversy (Berberian and King, 1981; Izzeldin, 1987; Sultan *et al*., 1992; Mohajjel *et al*., 2003; Ghasemi and Talbot, 2006; Navabpour *et al*., 2007; Dillek and Sandvol, 2009; Agard *et al*., 2011).

This study is focused on description of three different basic dykes in the northeast of Golpayegan area. Generation and magma evolution are discussed and geodynamic setting of these rocks is investigated. This study is also trying to estimate tectonic setting of Golpayegan area and SSZ on the base of the distinctive trace-element characteristics of different basic dykes. It will be useful in understanding the geodynamical evolution of Iran

2- Geological Setting

The Zagros fold and the thrust belt of SW-Iran are parts of the continental collision zones. This orogenic belt (Fig. 1) consists of four NW-SE trending parallel zones: (1) Urumieh-Dokhtar Magmatic Assemblage, (2) Sanandaj-Sirjan Zone, (3) High Zagros, and (4) Zagros Simply folded belt (Alavi, 1994). The study area is located at latitudes of 33˚, 34′ N to 33˚, 40′ N and longitudes of 50˚, 16.5′ E to 50˚, 32.5′ E (Fig. 2). As discussed, the study area is placed in SSZ which is a narrow belt that lies to the southwest of Urumieh-Dokhtar magmatic belt. The SSZ is separated from the NW-trending high mountains of the imbricated belt on the southwest by the Main Zagros thrust. The SSZ extends for 1500 km along strike from northwest (Sanandaj) to southeast (Sirjan) in western Iran. It is about in 150–200 km wide and consists mainly of late Proterozoic–Mesozoic meta-carbonates, schist, gneiss, and amphibolite that are cut by deformed to undeformed granitoid plutons (Berberian and King 1981; Mohajjel and Fergusson 2000; Moritz *et al*., 2006; Mazhari *et al*., 2009). Metamorphosed Triassic–Lower Jurassic volcano–sedimentary sequences within the SSZ are interpreted to represent rift-drift units associated with the early-stage evolution of the Southern Neotethys (Alavi and Mahdavi 1994; Mohajjel *et al*., 2003).

Middle Jurassic to Late Cretaceous, medium- to high-pressure metamorphism and deformation recorded in the SSZ rocks were related to the subduction of the Southern Neotethyan seafloor northeastwards beneath SSZ (Berberian and King 1981; Moritz *et al*., 2006). The general structural fabric is defined by NW-trending and SW-overturned folds, SW-vergent thrust faults, and NW-trending reverse faults that collectively resulted in crustal thickening in the SSZ. This contractional fabric was overprinted by regional-scale, right-lateral transpressional deformation as evidenced by a pervasive sub-horizontal stretching lineation and dextral shearing (Mohajjel & Fergusson 2000).

The oldest magmatic activity in the SSZ includes Late Proterozoic to Early Palaeozoic mafic rocks formed during extensional events (Berberian and King, 1981; Rachidnejad-Omran *et al*., 2002). Then Late Triassic and Early Jurassic tholeiitic mafic volcanic rocks (Alavi and Mahdavi, 1994), interpreted as remnants of Tethys oceanic crust (Mohajjel *et al*., 2003). Major magmatic episodes in the tectonic evolution of the SSZ are represented by widespread Late Jurassic–Cretaceous, calc-alkaline plutons intruded

into the crystalline basement, and by Eocene shoshonitic granitoids crosscutting all its structural fabric elements (Ghasemi and Talbot 2006; Mazhari *et al*., 2009). This Eocene magmatic pulse is coeval with the magmatism in the Urumieh–Dokhtar arc (or the Central Iranian Volcanic Belt) to the NE (Fig. 1). The westward extension of the SSZ is represented by the Puturge-Bitlis massif (B-P continental block) in southern Turkey.

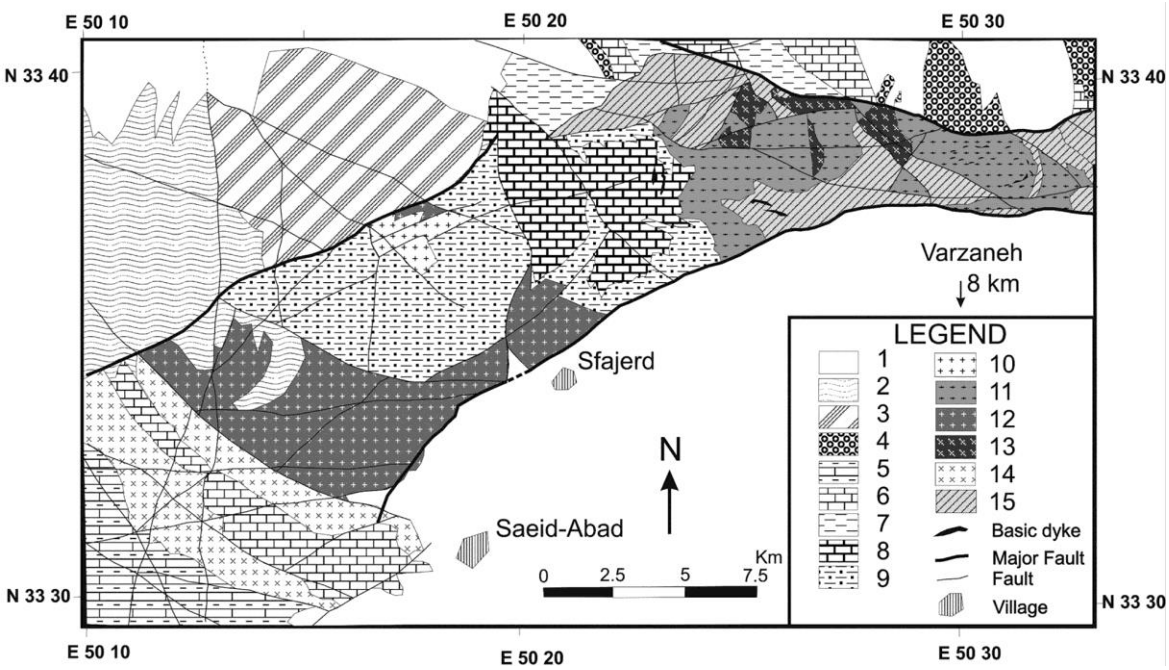

Figure 2) Geological map of the study area. 1-Recent alluvium, 2-Alluvial terraces, 3-Banding sandstone (Eocene), 4-Sandstone and conglomerate (Eocene), 5-Calcareous shale, Marl, Limestone (U. Cretaceous), 6-Orbitolina limestone (L. Cretaceous), 7-Shale (Jurassic), 8-Marble (Mesozoic), 9-Garnet muscovite schist (Mesozoic), 10-Monzogranite (Paleocene), 11-Mylonitic granite (Paleocene), 12-Syente, Syenodiorite (Paleocene), 13-Mylonitic basic rocks (M. Jurassic), 14-Trachyte (Cretaceous -Paleocene), 15-Meta-dacite, Meta-andesite, Meta-rhyolite (Mesozoic).

Although there is no unanimous agreement on the tectonic and geodynamic evolution in the SSZ, tectonic episode of SSZ may be outlined as following events. The Permian-Triassic extension produced the oceanic crust of the Neo-Tethys basin to the northeast of the present High Zagros Belt (Ricou, 1994). Stampfli and Borel (2002) pointed out that a subduction process started in the late Jurassic. Upper Cretaceous greenschist metamorphism and felsic granitoid plutons along the SSZ mark the continuation of subduction of Neo-Tethys along the western margin of the SSZ after the suturing of an intra-Neo-Tethys oceanic island arc to Arabia. The backarc basin behind this island arc was closing at a subduction zone dipping northwards beneath the Eurasian active margin by 65Ma (Robinson *et al*., 1995; Yilmaz *et al*. 1997; Rolland *et al*., 2009a, 2009b). These subduction-accretion systems in the northern part of the Neo-Tethys collapsed into the southern Eurasian margin by the early Eocene (Robinson *et al*., 1995).

The early Eocene was a time of regional contraction within the Neo-Tethys realm in the eastern Mediterranean region, and the

Gondwana-derived microcontinents were accreted along north-dipping subduction zones. The main collisions occurred in the northern and southern segments of the Neo-Tethys realm, near the Eurasia and Arabia continental plates respectively.

3- Materials and Methods

Measurements of whole rock major elements and trace elements were made at the ACME analytical laboratory in Canada. Six mylonitic gabbroic dyke samples were analyzed by XRF in which ten major element oxides and 24 trace elements were investigated. Seven other samples (samples SF-2, MA-3, GA-5, BA-2, SF-8, KH-12 and DR-3) were analyzed by the ICP-emission spectrometry for major elements and ICP-mass spectrometry (Perkin-Elmer Elan 600) for trace and rare earth elements.

3.2- Petrography and Geochemistry

Dykes in the northeast of the Golpayegan area can be petrographically divided in to three distinctive types as:

1- Mylonitic gabbroic dykes: samples of this group are foliated and mainly composed of plagioclase, pyroxene and hornblende.
2- Alkali dioritic and basanitic dykes.
3- Alkali monzogabbroic and monzodioritic dykes.

Samples group 2 and 3 are unfoliated dykes which normally cut their host rocks discordantly. The photomicrographs of samples are shown in Figure 3. Group 2 and 3 are chiefly composed of plagioclase, pyroxene and biotite. Groundmass biotite is altered to chlorite in most of samples, and feldspars are partially saussuritised in all samples (Fig. 3). The host rock of group 1 is mylonitic granite while the host rock of group 2 and 3 is granitic and syenitic-dioritic intrusions with age of about 55 Ma (Moritz et al., 2006).

Chemical compositions of the studied basic dykes, in the north of Golpayegan, including major and trace elements are presented in the Tables 1 and 2.

Samples of group 1 range in SiO_2 from 43.39 to 46.92 wt.% TiO_2 = 1.02-2.11 wt.%, Al_2O_3 = 13.12-16.16 wt.%, Fe_2O_3 = 3.71-5.23 wt.%, FeO= 5.55-7.85 wt.%, MgO = 6.70-10.75 wt.%, Cr_2O_3 = 0.031-0.049 wt.%, K_2O = 0.38 -2.82, Na_2O= 2.93-4.28 wt.%.

Samples of group 2 range in SiO_2 from 42.82 to 48.54 wt.% TiO_2 = 1.76-2.58 wt.%, Al_2O_3 = 15.40-17.54 wt.%, Fe_2O_3 = 3.08-4.56 wt.%, FeO= 6.54-7.73 wt.%, MgO = 5.05-7.13 wt.%, Cr_2O_3 = 0.01-0.03 wt.%, K_2O = 0.48-2.04, Na_2O= 3.65-4.93wt.%.

Samples of group 3 range in SiO_2 from 43.13 to 45.49 wt.% TiO_2 = 1.44-2.08 wt.%, Al_2O_3 = 16.12-18.27 wt.%, Fe_2O_3 = 3.77-5.01 wt.%, FeO= 7.23-8.79 wt.%, MgO = 4.81-8.99 wt.%, Cr_2O_3 = 0.007-0.037 wt.%, K_2O = 0.75-2.6, Na_2O= 2.27-3.31 wt.%.

The group 1 has amphibole that is why L.O.I of group 1 is higher than normal. None of the analysed samples is altered. Anyway trace elements used for classification. In Figure 4 Nb/Y versus Zr/TiO_2 diagram (Winchester and Floyd, 1977) is used for classification of the samples.

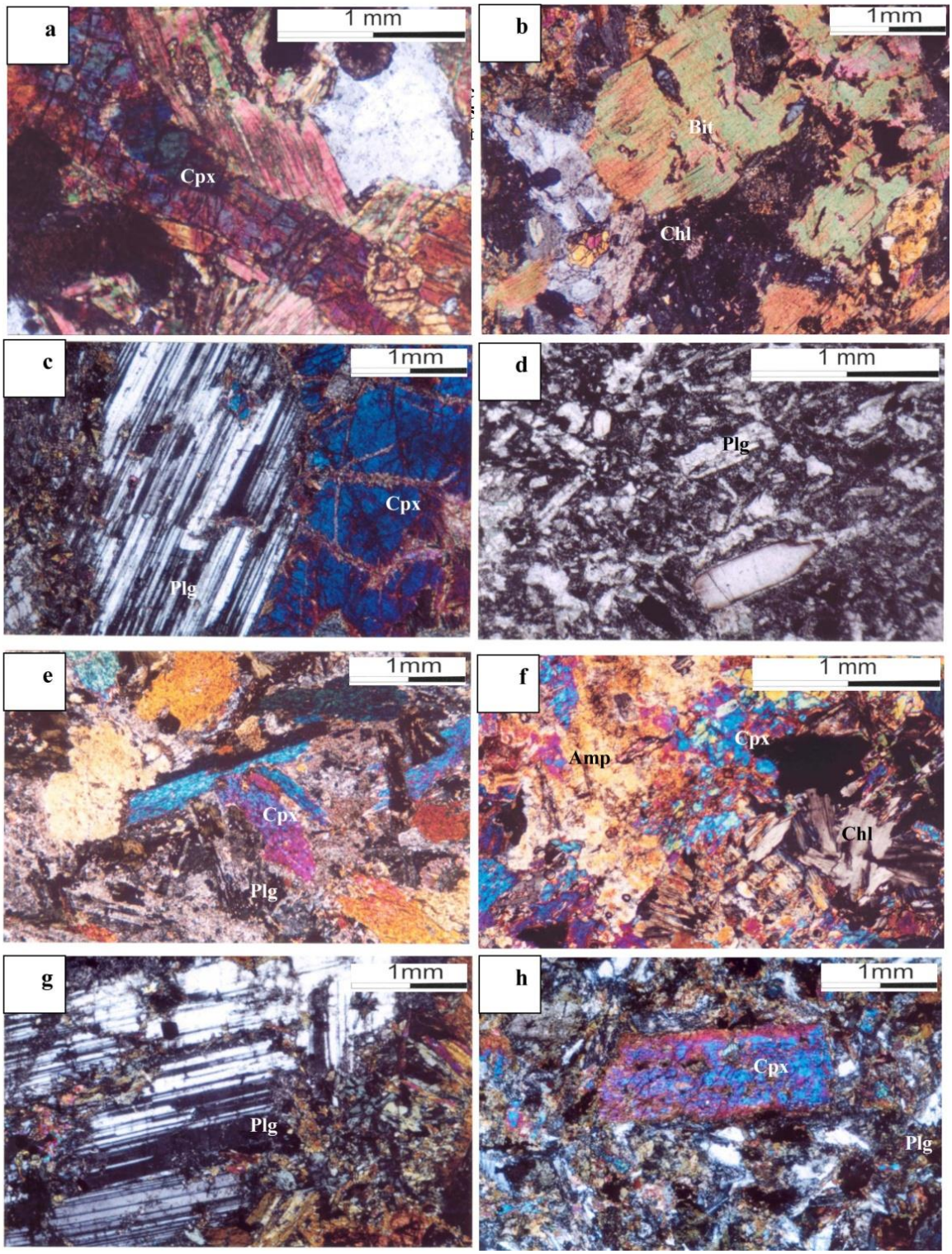

Figure 3) Photomicrograph of the basic dykes from the Golpayegan area. (a)- Nephelinemonzogabbro (sample Ga-5), (b)-Monzodiorite (sample Ba-2), (c)- gabbro (sample KH-2), (d)-Alkali basalt (sample Dr-1), (e)- Diorite (sample Ma-3), (f)- Monzogabbro (sample SF-8), (g)- Gabbro (sample KH-12), (h)- Hawaiite/ Phonolitictephrite (sample SF-2).

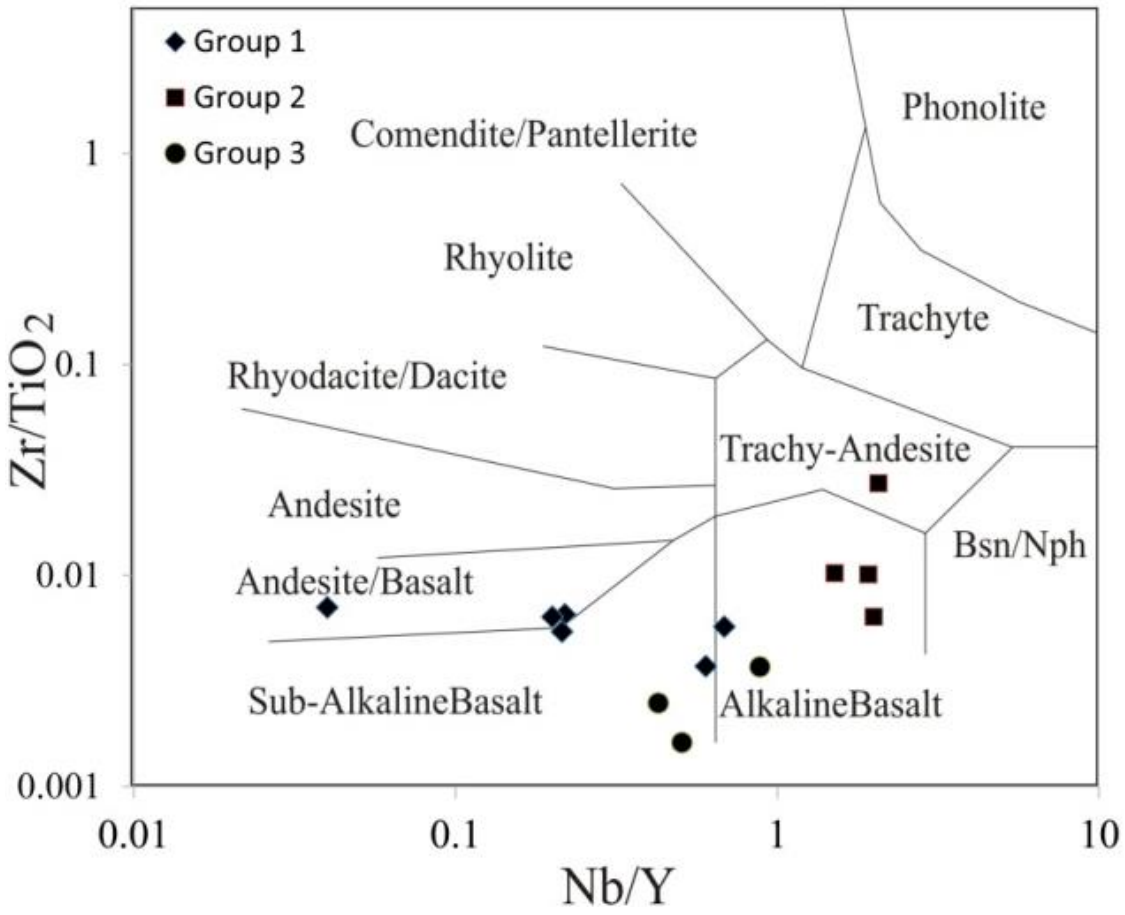

Figure 4) Nb/Y vs Zr/TiO_2 classification diagram (Winchester and Floyd, 1977).

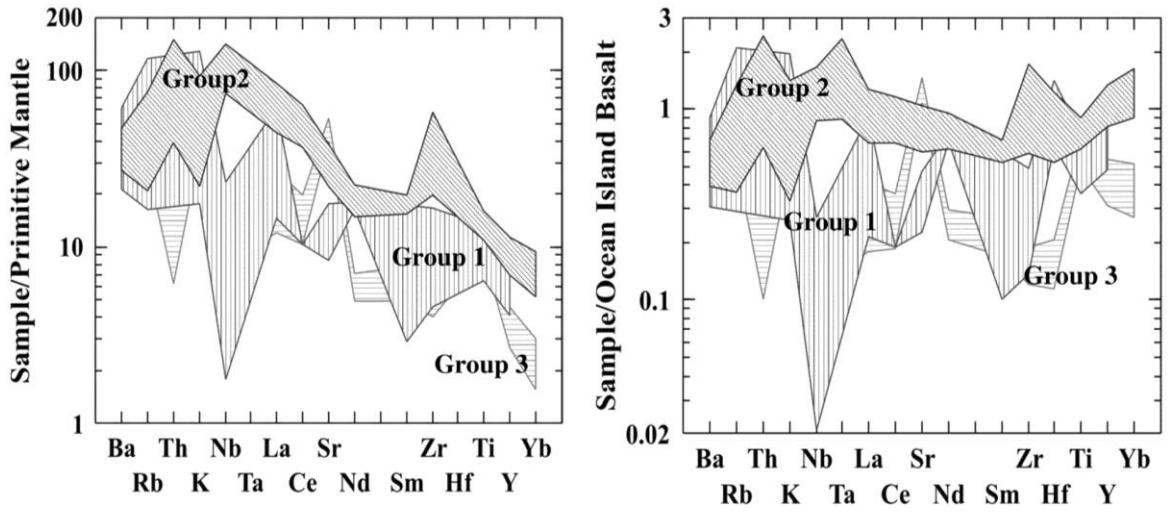

Figure 5) Spider diagrams normalized to primitive mantle and ocean island basalt (Sun and McDonough, 1989).

It shows that group 1 dykes occupy basaltic andesite and sublkaline basalt fields. Group 3 dykes plot in both sublakline and alkali baslatic fields. The group 2 dykes plot in alakli basaltic field and except one sample that is located in the trachy andesite field. Regarding K_2O/Na_2O ratio < 1 indicating sodic nature of group 2 (Jaques *et al*., 1985) together with presence of nepheline and the absence of acmite in the norm

support silica-undersaturated and alkaline nature (Middlemost, 1989) for group 2.

Spider diagrams normalized to primitive mantle (Sun and McDonough, 1989) and oceanic island basalt (Sun and McDonough, 1989) for studied rocks are displayed in Figure 5. This is also depicted in Figure 4 that group 2, having high concentration in high field strength elements (HFSE) such as Ta, Nb and Ti, is clearly separated from other groups. The high HFSE contents of the group 2 suggest that their source was significantly enriched in these elements stored in such minerals as garnet (implying asthenospheric mantle). Partition coefficient of HFSE for mineral/basalt is very low (Rollinson, 1993). That shows HFSE are very incompatible and have tendency to participate in basaltic melt. This clearly indicates that basaltic magmas enriched in HFSE were derived from an enriched source. This geochemistry behavior of HFSE such as Ti strongly supports the theoretical positive correlation between depth of source and content of Ti in magma. Compared with OIB, the study samples of group 2 have lower Ti concentrations (Fig. 5), implying that the initial magma was derived from a shallower depth rather than OIB (Yan and Zhao, 2008). Ti, as an incompatible element in upper mantle, does not tend to remain in the source.

All three groups of studied dykes have a specific range of content in HFSE. For group 1, 2 and 3 respectively, Zr ranges in 38-137, 164-480 and 33.5-53; Hf ranges in 5-11, 4.1-9.6 and 0.9-1.6; Nb ranges in 1-13, 41.5-79.5 and 4.6-10.6. For group1 and 2 respectively, Th ranges in 2.5-9.7 and 0.4-1.6. Ta ranges in 2.4-6.3 and 0.4-0.7. Having more high contents of incompatible elements in group 2 rather than group 3 signifies a more enriched source for group 2 than group 3. It is noticeable that Zr and Th usually are not mobile elements. This is why they are in petrogenesis diagrams. However, they may show mobility under the strong effect of rich-fluid matasomatism.

Table 1) XRF major elements (wt %) and trace elements (ppm) analyses of the studied samples from the mylonitic gabbros (Group 1).

Sample	O1	D5	BA-10	A8	A-3	A-12
SiO_2	46.92	45.54	43.39	44.74	45.05	45.35
TiO_2	1.027	1.905	1.876	1.055	2.112	2.1
Al_2O_3	16.16	13.12	13.25	14.72	14.35	13.35
Fe_2O_3	3.71	4.747	4.389	3.83	5.11	5.23
FeO	5.55	7.121	6.58	5.74	7.67	7.85
MnO	0.17	0.17	0.18	0.18	0.2	0.19
MgO	8.47	7.01	10.76	9.62	6.98	6.70
CaO	10.28	8.94	7.63	10.93	9.85	9.7
Na_2O	3.985	4.277	2.928	3.666	3.685	3.627
K_2O	0.48	0.79	2.82	0.46	0.38	0.38
P_2O_5	0.142	0.186	0.208	0.124	0.205	0.204
Cr_2O_3	0.049	0.038	0.045	0.03	0.031	0.031
Total	**97.5**	**94.55**	**94.72**	**95.67**	**96.4**	**95.5**
Ba	121	314	300	108	145	143
Rb	14	24	65	16	9	10
Sr	245	224	314	167	149	155
Ga	16	19	18	13	23	22
Nb	9	1	13	3	7	7
Hf	7	11	11	5	8	8
Zr	38	134	107	57	134	137
Y	15	25	19	14	35	32
Ni	88	59	240	160	70	60
Co	37	51	44	43	45	42
V	234	324	171	243	362	369
Cu	1	126	56	34	38	39
Pb	1	4	2	0	4	4
Zn	85	172	103	94	89	88
F	82	192	39	12	345	358
Cl	284	320	110	306	492	483
S	9	6	5	6	86	76
La	0	34	0	0	9	8
Ce	0	0	0	0	15	15
Zr/Y	2.533	5.36	5.632	4.071	3.829	4.281
Mg#	62.9	52.7	64.5	65.1	50.3	47
Ne Norm	5.67	5.2	8.4	7.65	2.42	0.86

That content of Zr and Th of samples widely varies show the role of fluid to metasomatic the mantle magma source. Considering that Cs is a highly mobile element (Tonarini *et al*., 2001), marked

enrichment in Cs relative to Rb suggests that the metasomatic agents were the fluid phases probably derived from the subducting slab (e.g. Rollinson, 1993; Shaw *et al*., 2003).

However, group 1 and 3 are signified by low contents in HFSE. The low concentration for the HFSE for example Nb and Ta are typical of rocks from subduction zones and they have been explained with a mantle source overprinted by fluids and melts from a subducting slab (Tatsumi and Kogiso, 1997). Chondrite-normalized and OIB-normalized REE patterns of the analyzed samples are shown in Figure 6. REE diagrams clearly segregate group 2 and 3 (Fig. 6).

REE patterns normalized to OIB (Fig. 6) indicate that rocks of group 2 are similar to oceanic island basalts, because the normalized values to OIB tend to be near 1. OIB normalized REE pattern show that group 2 is OIB-like, but not group 3.

The chondrite-normalized REE pattern of the analyzed samples (Fig. 6) show that group 2 and 3 are 4 to 130 times more enriched in REE than that in chondrite. In this diagram all samples present a negative slope for REE. All the studied rocks are enriched in light REE relative to heavy REE and exhibit smooth, inclined and parallel patterns and resemble those of mildly under saturated alkali basalts. Relatively low HREE contents of group 2 and 3 indicate that garnet was present as a residual phase in their mantle sources.

At the first glance to REE pattern diagram, discrimination between group 2 and 3 is conspicuous, because there is a wide gap between their patterns. Group 2 is much more enriched in REE than group 3. As it is obvious in Figure 6, the samples do not show negative Eu anomaly, even group 3 shows positive Eu anomaly. They represent that plagioclase did not have an important role in partial melting and magma evolution for group 2. It is possible that plagioclase was absent in the source of group 2, but not in group 3.

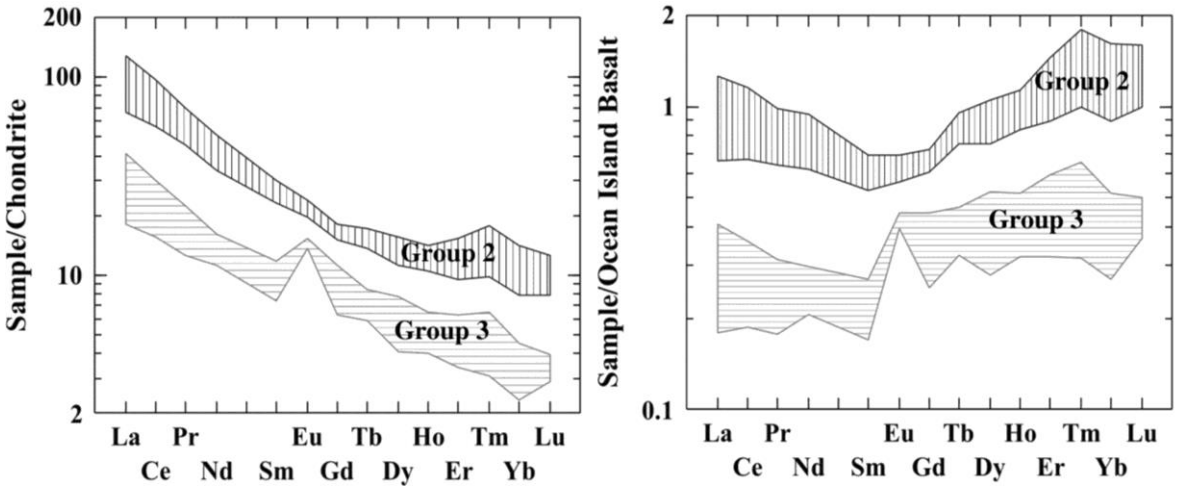

Figure 6) REE distribution patterns normalized to the chondrite (from Nakamura, 1974) and oceanic island basalt (Sun and McDonough, 1989).

4- Magma source and evolution

Plotting Th/Yb versus Ta/Yb (Wilson, 1989) indicates that basic dykes of group 2 and 3 have been derived from an enriched mantle source.

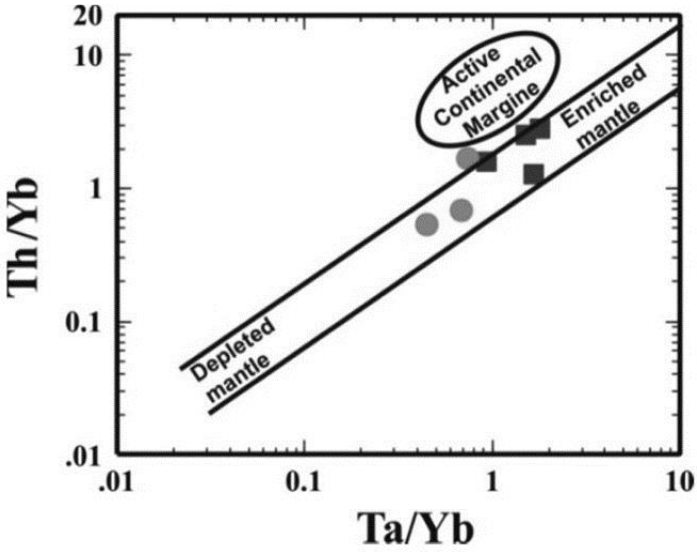

Figure 7) Th/Yb vs Ta/Yb diagram (Wilson, 1989) suggesting an enriched mantle source for the basic dykes from the Golpayegan area (symbols are same as Figure 4).

Figure 7 shows that the higher ratio of both Th/Yb and Ta/Yb is the more enriched source. Being more enriched in Ta and Yb, group 2 is derived from a more enriched source than group 3 (Fig. 7). Mantle source characteristics of the basic dykes (group 2 and 3) are evaluated in terms of Th/Y vs. Nb/Y plot (Fig. 8). These ratios are considered to be independent of the effects of fractional crystallization or partial melting and hence can be effectively used in a search for the mantle source characteristics (Özdermir *et al*., 2006).

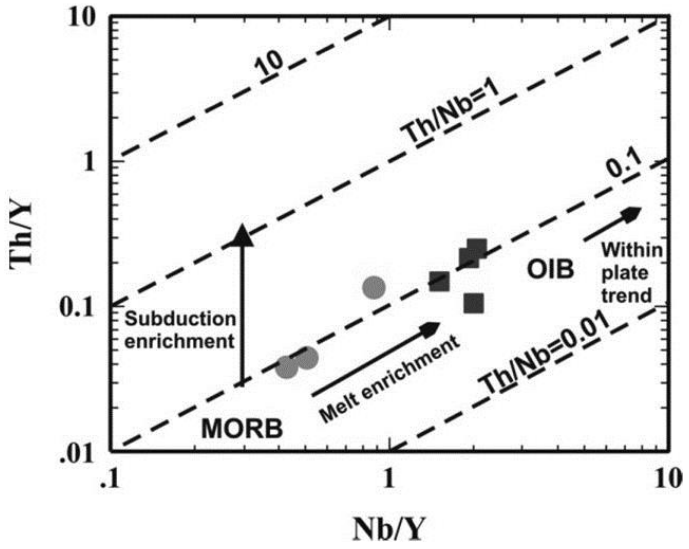

Figure 8) Th/Y vs. Nb/Y diagram for the basic dykes (Group 2 and 3, symbols are same as Figure 4). Data source: MORB and OIB fields and TH/Nb lines (Kempton et al., 1991).

A similar plot (Th/Yb vs Ta/Yb) was originally proposed by Pearce (1983) to discriminate the effects of subduction from the mantle components as the subduction component affects Th much more than Ta (and/or Nb), whereas within-plate enrichment events are characterised by an equal enrichment in Th and Ta (and/or Nb) (Pearce, 1983).

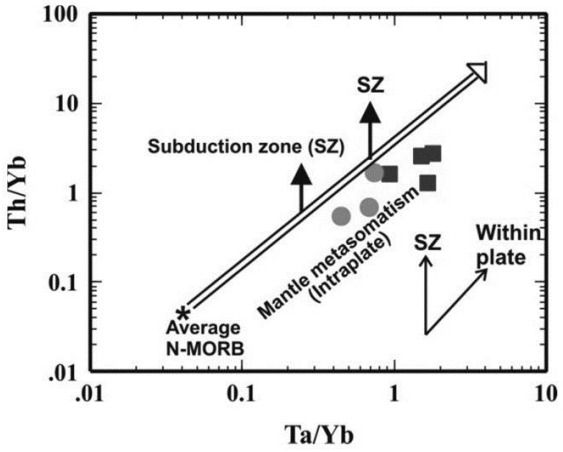

Figure 9) Th/Yb/Yb vs Ta/Yb (Pearce, 1983) for the basic dykes (Groups 2 and 3, symbols are same as Figure 4).

Studied samples are also plotted in a diagram of Th/Yb against Ta/Yb (Fig. 9). According to Figures 8 and 9, groups 2 and 3 both show within-plate enrichment trend and form trends that run parallel to the mantle metasomatism array (e.g. Pearce, 1983). Tectonic discrimination diagram for these rocks (Fig. 10) confirms that studied dykes have been occurred in a within-plate environment. Previously it is discussed that study area has undergone subduction processes, but it goes back to past events. It is also mentioned that group 2 and 3 rocks cut post-collisional rocks.

Therefore it is not antithetical that studied dykes show within-plate tectonic setting. The subducted slab had caused metasomatism in the upper mantle from which later magma forming dykes is derived.

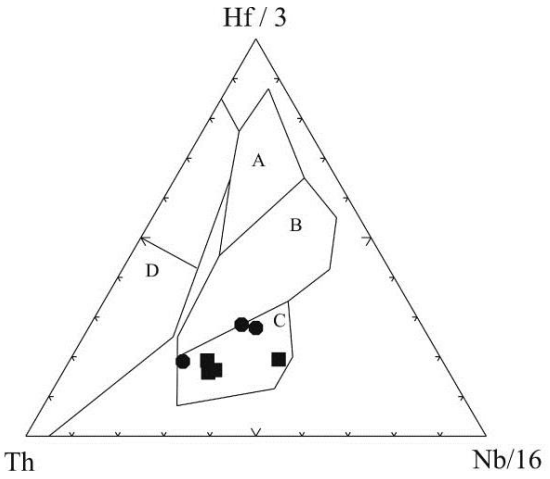

Figure 10) Discrimination geotectonic diagram for the group 2 and 3 of studied rocks (symbols are same as Figure 4)-Th-Hf/3-Ta triangle (Wood, 1980). A and B: N-type MORB, C: Within plate Alkaline basalts, D: Destructive plate-margin basalts.

On the base of what has been discussed so far, group 2 is within-plate alkaline basalt. The genesis of within-plate alkaline basalts is a matter of considerable debate. The following sources have been proposed for these SiO_2-unsaturated melts (Zeng *et al*., 2010): (1) silica-deficient eclogite and garnet pyroxenite representing, for example, residual crust in the asthenosphere (Hirschmann *et al*., 2003; Kogiso *et al*., 2003), (2) hornblendite produced by hydrous metasomatism (McKenzie and O'Nions, 1995; Niuand O'Hara, 2003; Pilet *et al*., 2004, 2005,2008), (3) carbonated peridotite (Hirose, 1997; Dasgupta *et al*., 2007; Sisson *et al*., 2009), and (4) mixed sources (Prytulak and Elliott, 2007; Liu *et al*., 2008; Chen *et al*., 2009; Dasgupta *et al*., 2010).

Table 2) Chemical composition of samples Groups 2 and 3 from the Golpayegan area, Major elements are in wt %, trace elements are in ppm, Au is in ppb.

	Sample	SiO_2	TiO_2	Al_2O_3	Fe_2O_3	FeO	MnO	MgO	CaO	Na_2O	K_2O	P_2O_5	Cr_2O_3	Total
Group 2	SF-2	46	1.76	17.54	4.56	6.8	0.17	5.1	9.9	4.02	1.9	0.45	0.015	99.83
	MA-3	43	2.03	16.22	3.31	7.7	0.17	6.6	7.2	3.65	0.8	0.53	0.021	99.94
	DR-3	43	2.58	16.98	3.08	7.2	0.09	7.1	5.7	4.93	0.5	0.59	0.031	99.85
	BA-2	49	1.98	15.4	4.37	6.5	0.19	5.9	7.6	4.1	2	0.04	0.01	99.91
Group 3	SF-8	43	1.44	16.12	3.77	8.8	0.19	9	11	2.27	0.8	0.26	0.007	99.91
	KH-12	45	2.08	18.27	4.83	7.2	0.14	4.8	11	3.18	1	0.15	0.016	99.93
	GA-5	44	1.84	16.98	5.01	7.5	0.15	5.1	10	3.31	2.6	0.22	0.037	99.9

	Sample	Ba	Rb	Sr	Cs	Ta	Nb	Hf	Zr	Y	Th	U	Ni	Co
Group 2	SF-2	209	41.7	684.4	1.4	6.3	79.5	9.6	480	38.5	9.7	3.3	43.7	33.6
	MA-3	179	20.3	395.2	1.1	3.2	46.9	4.9	205	24.4	5.3	1.4	56.1	34.6
	DR-3	139	11.4	484.6	6.2	3.2	47.1	4.1	164	23.6	2.5	0.8	113.8	39.5
	BA-2	242	33.6	546.9	1.8	2.4	41.5	4.6	202	27.5	4.1	0.8	46.4	38.2
Group 3	SF-8	161	16	765	7.3	0.7	10.6	1.6	53	12	1.6	0.4	41	50
	KH-12	184	24.1	713.8	8.1	0.4	4.6	0.9	34	9.1	0.4	0.1	42.4	39.8
	GA-5	171	56.8	959.1	63.8	0.5	6.7	1.4	46	15.7	0.6	0.3	28.8	42

	Sample	Sc	V	Cu	Pb	Sn	W	Mo	Be	Au	Sb	La	Ce	Pr
Group 2	SF-2	24	203	78.6	25.3	5	2.7	2.1	7	5.7	0.5	36.3	65.4	6.39
	MA-3	25	213	8.2	6.5	7	6.3	0.8	2	1.6	0.1	46.7	92.5	9.52
	DR-3	23	214	12.1	69.6	2	0.5	0.9	1	2.4	0.3	24.4	53.3	6.21
	BA-2	27	219	32.2	2.6	2	1.4	2.3	2	1.2	0.1	30.9	60.6	6.46
Group 3	SF-8	32	278	52	18	3	3.7	1.9	6	1.2	0.5	15.1	28.6	3.04
	KH-12	37	448	129.1	5.1	1	1.1	1.6	1	0.8	0.6	6.6	14.9	1.72
	GA-5	29	265	27.9	13.6	3	2	3.2	2	3	0.5	9.3	20.8	2.54

	Sample	Nd	Sm	Eu	Gd	Tb	Dy	Ho	Er	Tm	Yb	Lu	La/Lu	Zr/Y
Group 2	SF-2	24	5.7	1.78	5.45	1	5.89	1.2	3.8	0.63	3.5	0.48	75.63	12.470
	MA-3	36	6.9	2.07	5.51	0.9	4.45	0.9	2.3	0.36	2.1	0.31	150.7	8.381
	DR-3	27	5.6	1.73	5.12	0.8	4.23	0.9	2.4	0.35	1.9	0.3	81.33	6.941
	BA-2	24	5.3	1.69	4.61	0.8	5	1	2.8	0.41	2.6	0.37	83.51	7.353
Group 3	SF-8	11	2.6	1.19	2.68	0.4	2.25	0.4	1.1	0.16	1	0.14	107.9	4.417
	KH-12	7.9	1.7	1.29	1.92	0.3	1.55	0.3	0.8	0.11	0.6	0.11	60	3.681
	GA-5	11	2.7	1.33	3.4	0.5	2.94	0.6	1.6	0.23	1.1	0.15	62	2.904

	Sample	La/Yb	Ce/Yb	Mg#	Ne Norm
Group 2	SF-2	10	18.7	43	8.96
	MA-3	22	44.1	52.2	1.75
	DR-3	13	27.5	56	5.69
	BA-2	12	23.7	50	3.28
Group 3	SF-8	16	30.1	56.7	3.77
	KH-12	11	25.7	40.5	2.12
	GA-5	8.3	18.6	41	11.1

According to total alkalis against TiO_2 plot shown in Figure 11 (Zeng *et al*., 2010), dykes of group 2 have been derived from a carbonated peridotite source which is a kind of metasomatised peridotite.

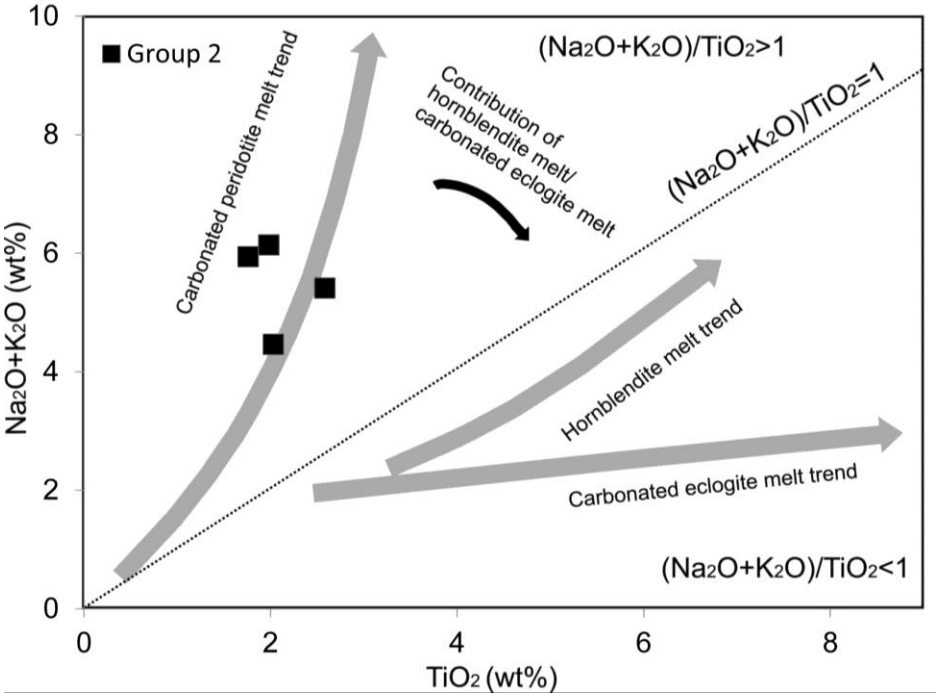

Figure 11) TiO_2 vs Total alkalis diagram (Zeng et al., 2010) and situation of studied samples

Highly incompatible elemental ratios can be used to trace petrogenetic processes. For instance, the Zr/Y ratio generally remains constant during fractional crystallization, but varies during partial melting in basaltic systems.

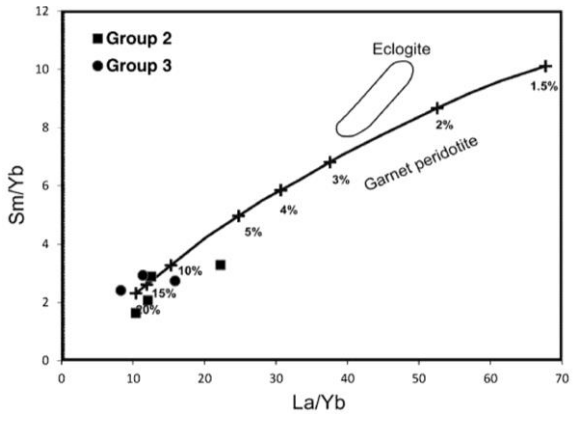

Figure 12) Sm/Yb vs La/Yb diagram for group 2 and 3 (Feigenson et al., 2003; Zeng et al., 2010).

Zr is more incompatible than Y in the mantle, so Zr/Y ratios tend to be higher in small degrees of partial melting and vice versa (Pearce & Norry, 1979; Nicholson & Latin, 1992). The group 1 and 2 have low Zr/Y ratios (2.5–5.6 and 2.9–4.4 respectively), but Zr/Y ratios in group 3 are higher than those of group1 and 2 (6.9–12.4). By applying these characteristics, partial melting can be estimated relatively. These features suggest that the degree of partial melting is lower for group 2 dykes as compared to group 1 and 3 dykes. To estimate the degree of partial melting in quantity the diagram of La/Yb versus Sm/Yb (Feigenson *et al*., 2003; Zeng *et al*., 2010) is used (Fig. 12). This diagram quantifies about 7–20% partial melting for group 2 and 12-20% partial melting for group 3.

5- Conclusions

Based on the trace-element chemistry, the basic dykes in the northeast of the Golpayegan area can be geochemically subdivided into three distinctive groups. The group 1 and 3 rocks are mainly subalkaline and group 2 rocks are alkaline. Samples of group 2 and 3 derived from an enriched mantle source. Group 2 is more enriched in HFSE, LILE and REE indicating that its source should be more enriched than groups of 1 and 3.

The deeper is the magma source the less depleted is the source and more magma becomes enriched in incompatible elements. Regarding the positive correlation between depth of magna source in upper mantle and content of HFSE, It seems magma forming rocks of group 2 was derived from deeper mantle than two other groups. It is probable that magma forming dykes of group 2 is possibly derived from an asthenospheric mantle, but two other groups were formed by magmas obtained from a lithospheric mantle.

The source of magma forming group 2 and 3 was maybe a metasomatised peridotite. According to chondrite normalized REE patterns (discussed in geochemistry section), garnet is present in residual during partial melting of the peridotite mantle. Plagioclase should have contributed in partial melting process only for magma forming group 3, but not group 2. This fact can be ratified by considering a shallower depth for partial melting for group 3. When studied samples are plotted in the discriminating tectonic setting diagrams, they show within-plate character. This does not make sense to expect that within plate magmatism should never occur in the lands that formerly have experienced subduction. Because the age of the group 2 and 3 studied dykes is related to the time after subduction, all the effects of metasomatism occurred on the wedge mantle above subducted slab is responsible for geochemistry behavior of studied dykes. The subduction of Neo-Tethys may be the potential cause of enrichment of the mantle and next alkaline magmatism (at least group 2) in Cenozoic. Greya *et al*. (2002) discussed that it takes at least 24 million years for the mantle to become metasomatised by subduction. Therefore, the subduction of Neo-Tethys from middle Jurassic to at least early Eocene may be enough for mantle enrichment in volatiles and next alkaline magmatism in Golpayegan area.

Acknowledgments

The authors would like to thank Prof. Tahseenullah Khan and Dr. Mehdi Rezaei Kahkhaei for their comments that help improve the manuscript. We also thank the University of Isfahan for its financial support.

References

Agard, P., Omrani, J., Jolivet, L., Whitechurch, H., Vrielynck. B., Spakman, W., Monie, P., Meyer, B.,Wortel, R. 2011. Zagros orogeny: a subduction-dominated process. Geological Magazine: 148, 692–725.

Alavi, M. 1994. Tectonics of the Zagros orogenic belt of Iran, new data and interpretations. Tectonophysics: 229, 211–238.

Alavi, M., Mahdavi, M.A. 1994. Stratigraphy and structure of the

Nahavand region in western Iran and their implications for the Zagros tectonics. Geological Magazine: 131, 43-47.

Berberian, M., King, G.C.P. 1981. Toward a paleogeography and tectonic evolution of Iran. Canadian Journal of Earth Science: 18, 210-265.

Coban, H. 2007. Basalt Magma Genesis and Fractionation in Collision and Extension Related Provinces: A Comparison between Eastern, Central and Western Anatolia. Earth Science: 80, 219-238.

Chen, L.H., Zeng, G., Jiang, S.Y., Hofmann, A.W., Xu, X.S. 2009. Sources of Anfengshan basalts: subducted lower crust in the Sulu UHP belt, China. Earth and Planetary Science Letters: 286, 426–435.

Dasgupta, R., Hirschmann, M.M., Smith, N.D. 2007. Partial melting experiments of Peridotitie+CO_2 at 3 GPa and genesis of alkalic ocean island basalts. Journal of Petrology: 48, 2093–2124.

Dasgupta, R., Jackson, M.G., Lee, C.T. 2010. Major element chemistry of ocean islandbasalts- conditions of mantle melting and heterogeneity of mantle source. Earth and Planetary Science Letters: 289, 377–392.

Dilek, Y., Sandvol, E. 2009. Seismic structure, crustal architecture and tectonic evolution of the Anatolian-African plate boundary and the Cenozoic orogenic belts in the eastern Mediterranean region. Geological Society of London. Special Publication: 327, 127–160.

Feigenson, M.D., Bolge, L.L., Carr, M.J., Herzberg, C.T. 2003. REE inverse modeling of HSDP2 basalts: evidence for multiple sources in the Hawaiian plume. Geochemistry, Geophysics, Geosystems: doi:10.1029/2001gc000271.

Gerya, T.V., Perchuk, L.L., Maresch, W.V., Willner, A.P., Van Reenen, D.D., Smit, C.A. 2002. Thermal Regime and Gravitational Instability of Multi-Layered Continental Crust: Implications for the Buoyant Exhumation of High Grade Metamorphic Rocks. European Journal of Mineralogist: 14, 687–699.

Ghasemi, A., Talbot, C.J. 2006. A new tectonic scenario for the Sanandaj-Sirjan zone (Iran). Journal of Asian Earth Sciences: 26, 683-693.

Hirose, K. 1997. Partialmelt compositions of carbonated peridotite at 3 GPa and role of CO2 in alkali–basalt magma generation. Geophysical Research Letters: 24, 2837–2840.

Hirschmann, M.M., Kogiso, T., Baker, M.B., Stolper, E.M. 2003. Alkalic magmas generated by partial melting of garnet pyroxenite. Geology: 31, 481–484.

Izzeldin, A.Y. 1987. Seismic, gravity and magnetic survey in the central part of the Red sea, their interpretation and implications for the structure and evolution of the Red sea.Tectonophysics: 143, 264-306.

Jaques, A.L., Creaser, R.A., Ferguson, J., Smith, C.B. 1985. A review of the Alkaline Rocks of Australia. Geological Society of South Africa: 88, 311–334.

Kempton, P.D., Fitton, J.G., Hawkesworth, C.J., Ormerod, D.S. 1991. Isotopic and trace element constraints on the composition and evolution of the

lithosphere beneath the southwestern United States. Journal of Geophysical Research: 96, 13713-13735.

Kogiso, T., Hirschmann, M.M., Frost, D.J. 2003. High-pressure partial melting of garnet pyroxenite: possible mafic lithologies in the source of ocean island basalts. Earth and Planetary Science Letters: 216, 603–617.

Liu, Y.S., Gao, S., Kelemen, P.B., Xu, W.L. 2008. Recycled crust controls contrastingsource compositions of Mesozoic and Cenozoic basalts in the North China Craton. Geochimica et Cosmochimica Acta: 72, 2349–2376.

Mazhari, S.A., Bea, F., Amini, S., Ghalamghash, J., Molina, J.F., Montero, P., Scarrow, J.H., Williams, I.S. 2009. The Eocene bimodal Piranshahr massif of the Sanandaj–Sirjan Zone, NW Iran: A marker of the end of the collision in the Zagros orogeny. Journal of the Geological Society of London: 166, 53–69.

McKenzie, D.A.N., O'Nions, R.K. 1995.The source regions of ocean island basalts. Journal of Petrology: 36, 133–159.

Middlemost, E.A.K. 1989. Iron Oxidation Ratios, Norms and the Classification of Volcanic Rocks. Chemical Geology: 77, 19–26.

Mohajjel, M., Fergusson, C.L. 2000. Dextraltranspression in Late Cretaceous continental collision, Sanandaj-Sirjan Zone, western Iran. Journal of Structural Geology: 22, 1125-1139.

Mohajjel, M., Fergusson, C.L., Sahandi, M.R. 2003. Cretaceous-Tertiary convergence and continental collision, Sanandaj-Sirjan Zone, western Iran. Journal of Asian Earth Sciences: 21, 397-412.

Moritz, R., Ghazban, F., Singer, B.S. 2006. Eocene gold ore formation at Muteh, Sanandaj-Sirjan tectonic zone, Western Iran: A result of late-stage extension and exhumation of metamorphic basement rocks within the Zagros Orogen. Economic Geology: 101, 1497-1524.

Nakamura, N. 1974. Determination of REE, Ba, Fe, Mg, Na and K in carbonaceous and ordinary chondrites. Geochimica et Cosmochimica Acta: 38, 757-775.

Navabpour, P., Angelier, J., Barrier, E. 2007. Cenozoic post-collisional brittle history and stress recorientation in the High Zagros Belt (Iran, fars province). Tectonophysics: 423, 101-131.

Nicholson, H., Latin, D. 1992. Olivine Tholeiites from Krafla, Iceland: Evidence for Variations in the Melt Fraction within a Plume. Journal of Petrology: 33, 1105-1124.

Niu, Y., O'Hara, M.J. 2003. Origin of ocean island basalts: a new perspective from petrology, geochemistry, and mineral physics considerations. Journal of Geophysical Research: 108, 2209–2228.

Özdermir, Y., Karaoğlu, Ö., Tolluoglu, A.Ü., Güleç N. 2006. Volcano-stratigraphy and petrogenesis of the Nemrutstratovolcano (East Anatolian High Plateau). The most recent post-collisional volcanism in Turkey. Chemical Geology: 226, 189-211.

Pearce, J.A. 1983. Role of the sub-continental lithosphere in magma genesis at active continental margins, in: Hawkesworth, C.J. Norry, M.J. (Eds.),

Continental Basalts and Mantle Xenoliths, Shiva Publication, 230-249.

Pearce, J.A., Norry, M.J. 1979. Petrogenetic implications of Ti, Zr, Y and Nb variations in volcanic rocks. Contribution to Mineralogy and petrology: 69, 33–47.

Pilet, S., Hernandez, J., Bussy, F., Sylvester, P.J. 2004. Short-term metasomatic control of Nb/Th ratios in the mantle sources of intraplate basalts. Geology: 32, 113–116.

Pilet, S., Hernandez, J., Sylvester, P., Poujol, M. 2005. Themetasomatic alternative forocean island basalt chemical heterogeneity. Earth and Planetary Science Letters: 236, 148–166.

Pilet, S., Baker, M.B., Stolper, E.M. 2008. Metasomatised lithosphere and the origin of alkaline Lavas. Science: 320, 916–919.

Prytulak, J., Elliott, T. 2007. TiO_2 enrichment in ocean island basalts. Earth and Planetary Science Letters: 263, 388–403.

Rachidnejad-Omran, N., Emami, M.H., Sabzehei, M., Rastad, E., Bellon, H., Piqué, A. 2002. Lithostratigraphieet histoire paléozoïque à paléocène des complexes métamorphiques de la région de Muteh, zone de Sanandaj-Sirjan (Iran méridional). Geoscience: 334, 1185-1191.

Ricou, L.E. 1994, Tethys reconstructed: plates, continental fragments and their boundaries since 260 Ma from Central America to Southeastern Asia. Geodinamica Acta, 7, 169–218.

Robinson, A.G., Banks, C.J., Rutherford, M.M., Hirst, J.P.P. 1995. Stratigraphic and structural development of the Eastern Pontides, Turkey. Journal of the Geological Society of London: 152, 861–872.

Rolland, Y., Billo, S., Corsini, M., Sosson, M., Galoyan, G. 2009a. Blueschists of the Amassia-Stepanavan Suture Zone (Armenia): Linking Tethys subduction history from E-Turkey to W-Iran. International Journal of Earth Sciences: 98, 533–550.

Rolland, Y., Galoyan, G., Bosch, D., Sosson, M., Corsini, M., Fornari, M., Verati, C. 2009b. Jurassic back-arc and Cretaceous hot-spot series in the Armenian ophiolites – Implications for the obduction processes. Lithos: 112, 163-187.

Rollinson, H.R. 1993. Using Geochemical Data: Evaluation, Presentation, Interpretation: Longman, U.K., pp. 352.

Sisson, T.W., Kimura, J.I., Coombs, M.L. 2009. Basanite–nephelinite suite from early Kilauea: carbonated melts of phlogopite–garnet peridotite at Hawaii's leading magmatic edge. Contributions to Mineralogy and Petrology: 158, 803–829.

Sharifi, M. 2008, Investigation of alkaline magmatism in the north of Golpayegan area. Ph.D. thesis, University of Isfahan, Iran.

Shaw, A.M., Hilton, D.R., Fischer, T.P., Walker, J.A., Alvarado, G.E. 2003. Contrasting He–C relationships in Nicaragua and Costa Rica: Insights into C Cycling through Subduction Zones. Earth and Planetary Science Letters: 214, 499–513.

Stampfli G., Borel G.D. 2002. A plate tectonic model for the Paleozoic and

Mesozoic constrained by dynamic plate boundaries and restored synthetic oceanic isochrones. Earth and Planetary Science Letters: 196, 17–33.

Sultan, M., Becker, R., Arvidson, R.E., Sore, P., Stern, N.J., Al-Alfy Z., Guinness, A. 1992. Nature of Red Sea crust, a controversy revisited. Geology: 20, 593-596.

Sun, S.S., McDonough, W.F. 1989. Chemical and isotopic systematics of oceanic basalts: Implications for mantle composition and processes, In: Saunders, A.D., Norry, M.J. (Eds.), Magmatism in the ocean basins, Geological Society, London, Special Publications, 313-345.

Tang, Y.J., Zhang, H.F., Ying, J.F., 2006, Asthenosphere Lithospheric Mantle Interaction in an Extensional Regime: Implication from the Geochemistry of Cenozoic Basalts from Taihang Mountains, North China Craton. Chemical Geology: 233, 309–327.

Tatsumi, Y., Kogiso T. 1997. Trace element transport during dehydration processes in the subducted oceanic crust: 2. Origin of chemical physical characteristics in arc magmatism. Earth and Planetary Science Letters: 148, 207-221.

Tonarini, S., Armienti, P., D'orazio, M., Innocenti, F. 2001. Subduction_Like Fluids in the Genesis of Mt. Etna Magmas: Evidence from Boron Isotopes and Fluid Mobile Elements. Earth and Planetary Science Letters: 192, 471–483.

Turner, S., Hawkesworth, C. 1995. The Nature of the Sub Continental Mantle: Constraints from the Major Element Composition of Continental Flood Basalts. Chemical Geology: 120, 295–314.

Wilson, M. 1989. Igneous petrogenesis: A global tectonic approach, Unwin and Hyman, London.

Wood, D.A. 1980. The Application of a Th–Hf–Ta Diagram to Problems of Tectonomagmatic Classification. Earth and Planetary Science Letters: 50, 1–30.

Yan, J., Zhao, J.X. 2008, Cenozoic Alkali Basalts from Jingpohu, NE China: The Role of Lithosphere–Asthenosphere Interaction. Journal of Asian Earth Science: 33, 106–121.

Yilmaz, Y., Tüysüz, O., Yigitbas, E., Genc¸, S.C., Sengor, A.M.C. 1997. Geology and tectonic evolution of the Pontides, in Robinson, A.G., ed., Regional and Petroleum Geology of the Black Sea and Surrounding Region. American Association of Petroleum Geologists: 68, 183–226.

Zeng, G., Chen, L.H., Xu, X.S., Jiang, S.Y., Hofmann, A.W. 2010. Carbonated Mantle Sources for Cenozoic Intra Plate Alkaline Basalts in Shandong, North China. Chemical Geology: 273, 35-45.